Available online at www.sciencedirect.com
ScienceDirect
Journal of Sound and Vibration 318 (2008) 565–579
JOURNAL OF SOUND AND VIBRATION
www.elsevier.com/locate/jsvi

Modal stability of inclined cables subjected to vertical support excitation

A. Gonzalez-Buelga, S.A. Neild*, D.J. Wagg, J.H.G. Macdonald

Faculty of Engineering, University of Bristol, Queens Building, University Walk, Bristol BS8 1TR, UK

Received 27 November 2007; received in revised form 31 March 2008; accepted 14 April 2008
Handling Editor: M.P. Cartmell
Available online 6 June 2008

Abstract

In this paper the out-of-plane dynamic stability of inclined cables subjected to in-plane vertical support excitation is investigated. We compute stability boundaries for the out-of-plane modes using rescaling and averaging methods. Our study focuses on the 2:1 internal resonance phenomenon between modes that occurs when the excitation frequency is twice the first out-of-plane natural frequency of the cable. The second in-plane mode is excited directly, while the out-of-plane modes can be excited parametrically. An analytical model is developed in order to study the stability regions in parameter space. In this model we include nonlinear coupling effects with other modes, which have thus far been omitted from previous models of parametric excitation of inclined cables. Our study reflects the importance of such effects. Unstable parameter regions are defined for the selected cable configuration. The validity of the proposed stability model was tested experimentally using a small-scale cable actuator rig. A comparison between experimental and analytical results is presented in which very good agreement with model predictions was obtained.

1. Introduction

Cable-supported structures such as cable-stayed bridges are susceptible to vibration problems since they are relatively flexible and lightly damped. Cable dynamics can be strongly nonlinear, with internal coupling between modes and parametric coupling with external effects, such as the deck dynamics in the case of a cable-stayed bridge. These nonlinear effects can produce complex behaviour resulting in large amplitude cable vibrations; see for example the review by Nayfeh and Pai [1]. Parametric excitation can occur at specific ratios of excitation frequency to cable natural frequency, the most significant of which occurs at the 2:1 ratio, at which small excitation amplitudes at the cable anchorage can result in very large cable vibrations [2]. These vibrations can occur in-plane (defined as the plane in which the cable sags statically) or out-of-plane, even if the anchorage excitation is limited to just the in-plane direction, which is generally the dominant direction when a cable-stayed bridge cable is excited by deck motion.

*Corresponding author. Tel.: +44 117 928 9730; fax: +44 117 929 4423.
E-mail address: simon.neild@bristol.ac.uk (S.A. Neild).

0022-460X/$ - see front matter © 2008 Elsevier Ltd. All rights reserved.
doi:10.1016/j.jsv.2008.04.031

It has been shown that, provided sag is small, the second in-plane and out-of-plane cable natural frequencies are twice the first out-of-plane natural frequency although the first in-plane mode is slightly detuned due to cable sag [3]. If the lower support experiences vertical motion close to 2:1 resonance of the first out-of-plane mode it will directly excite the second in-plane mode. Due to cable nonlinearity, the motion of the second in-plane mode and the external excitation may, if the excitation is of sufficient amplitude, induce internal resonance in either the first or the second out-of-plane cable modes or both modes. This paper concentrates on determining the level of vertical excitation of the lower cable support required for the onset of an internally excited out-of-plane response. We refer to the onset of an out-of-plane response as the instability point of the semi-trivial solution—the solution where only the second in-plane mode is excited.

Modal stability studies of cable dynamics that consider parametric excitation were usually based on the Mathieu or Hill equation [4,5] without including nonlinear interaction between modes. The response in a single cable mode has been considered, see for example Refs. [2,6,7]. The study presented by Takahashi [8] included more than one mode of vibration but without modal coupling and so the problem reduces to uncoupled Mathieu equations. Other studies have considered autoparametric resonance of an inclined cable interacting with a beam, including nonlinearities, but only including a single in-plane mode [9,10]. An alternative cable-deck model proposed by Georgakis et al. [11] and developed by Lorenzo [12] allows for autoparametric resonance and nonlinearities and includes multiple cable modes, but has only been solved by numerical simulation.

Simulation studies which include modal coupling between in-plane and out-of-plane modes of sagging cables have been reported in Refs. [13–19]. Experimental studies of this problem have been conducted by Alaggio and Rega [20 and Rega and Allagio [21], however explicit stability regions for the semi-trivial solution have not been calculated analytically. Here, we use a modal model to compute the instability boundary for a range of excitation frequencies close to the 2:1 resonance for an inclined cable, including nonlinear modal interaction. For a specific excitation frequency, the point of instability is found by considering the local stability of the out-of-plane modes about zero amplitude response as the excitation amplitude increases. The point at which local out-of-plane modal instability occurs indicates the onset of oscillations for that mode and hence the semi-trivial solution is no longer valid.

The analysis was validated against an experimental set-up, consisting of an inclined cable attached to an electro-mechanic actuator, such that the lower anchorage point can be excited vertically. The cable displacements were tracked using a high-speed vision system [22]. The points of instability of the semi-trivial solution are detected in the experiment by looking for the onset of oscillations in the out-of-plane modes. The first in-plane mode is less susceptible to internal resonance when the excitation is at approximately twice the first out-of-plane frequency as the modal frequency is higher than the first out-of-plane frequency due to the cable sag [3]. However as the excitation frequency increases this mode may also be excited. Consideration of this mode is beyond the scope of the present study but the frequencies at which this mode is excited are identified in the experimental results.

In Section 2 a theoretical study of the stability of the semi-trivial solution is presented. The accuracy of the theoretical results are assessed in Section 3 by testing a small-scale cable both in simulation and experimentally. A comparison of the new model with existing models is discussed in Section 4 and conclusions are drawn in Section 5.

2. Theoretical study

Firstly we present a modal model of the cable dynamics [23]. When the excitation is close to twice the first out-of-plane natural frequency, the second in-plane mode is directly excited close to resonance. In addition to this the first and second out-of-plane modes may be excited parametrically or via nonlinear modal coupling. We therefore reduce the model to these three modes of interest.

Considering the modes of interest, the second step in the analysis is to scale the equations and introduce detuning in the excitation frequency to allow a study in the region around 2:1 resonance. We perform first-order averaging to derive differential equations of the response amplitudes for the sine and cosine components of the three modes. In the third step of the analysis we use these equations to assess the local stability at the zero amplitude point for the two out-of-plane modes in the presence of the external excitation and in-plane

motion. For either of the out-of-plane modes, local instability at the zero amplitude point will result in a response in that mode and hence mark the stability boundary of the semi-trivial solution. Finally, we consider the amplitude of response of the second in-plane mode just below the stability boundary of the semi-trivial solution and use this to derive a relationship between the excitation amplitude and frequency detuning parameter at the semi-trivial solution stability boundary. These stability boundaries are plotted in parameter space to indicate regions of stability and instability for each mode similar to plotting Arnold tongues for a single-degree-of-freedom Mathieu equation [5].

2.1. Step 1—Equations of motion

There have been many presentations of the equations of motion for cables [1]. In this paper we adopt the modal equations derived by Warnitchai et al. [23] for inclined cables with small sag. Their derivation includes the effects of support motion at both ends of the cable and accounts for cubic nonlinearities. The cable is supported at end points a and b and the direction of the chord line from a to b is defined as x, see Fig. 1. The cable equilibrium sag position and the chord line both lie in the $x-z$ plane, therefore z represents in-plane motion and y represents out-of-plane motion. The angle of inclination of the chord line relative to the horizontal is defined as θ. Following Warnitchai et al. [23], the modal representation of the out-of-plane cable motion may be expressed as

$$m_{yn}(\ddot{y}_n + 2\xi_{yn}\omega_{yn}\dot{y}_n + \omega_{yn}^2 y_n) + \sum_k \nu_{nk} y_n (y_k^2 + z_k^2) + \sum_k 2\beta_{nk} y_n z_k + 2\eta_n(u_b - u_a)y_n + \zeta_n(\ddot{v}_a + (-1)^{n+1}\ddot{v}_b) = F_{yn} \quad (1)$$

and the in-plane cable motion as

$$m_{zn}(\ddot{z}_n + 2\xi_{zn}\omega_{zn}\dot{z}_n + \omega_{zn}^2 z_n) + \sum_k \nu_{nk} z_n (y_k^2 + z_k^2) + \sum_k 2\beta_{nk} z_n z_k + \sum_k \beta_{kn}(y_k^2 + z_k^2) + 2\eta_n(u_b - u_a)z_n + \zeta_n(\ddot{w}_a + (-1)^{n+1}\ddot{w}_b) - \alpha_n(\ddot{u}_b - \ddot{u}_a) = F_{zn} \quad (2)$$

where y_n and z_n are the generalised displacements of the cable in the nth out-of-plane and in-plane modes, respectively; subscripts a and b denote the top and bottom anchorage points, respectively; $m_{yn} = m_{zn} = m$ is the effective mass ($m = \rho AL/2$); L is the cable length; σ_s is the cable static stress; λ^2 is Irvine's parameter [3], A is the cross-sectional area, ρ is the density, g is gravity and E is Young's modulus. The equivalent modulus of the cable E_q, the distributed weight perpendicular to the cable cord γ, and the parameters k_n, ν_{nk}, β_{nk}, η_n, ζ_n,α_n, λ^2, and F_{yn} and F_{zn} which represent external cable loading in the y and z direction, respectively, are given by

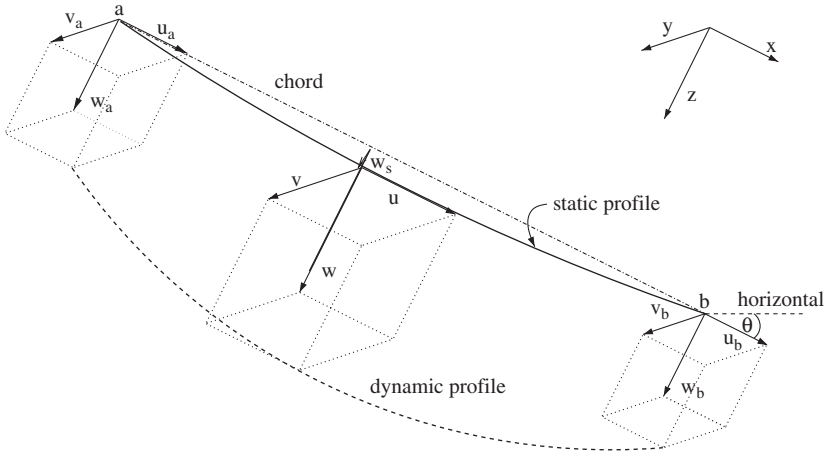

Fig. 1. Definition of cable coordinate system.

Warnitchai et al. [23]:

$$E_q = \frac{1}{1+\lambda^2/12}E, \quad \gamma = \rho g \cos\theta, \quad \lambda^2 = \frac{E}{\sigma_s}\left(\frac{\gamma L}{\sigma_s}\right)^2$$

$$v_{nk} = \frac{EA\pi^4 n^2 k^2}{8L^3}, \quad \beta_{nk} = \frac{EA\pi\gamma n^2}{4L\sigma_s}\left(\frac{1+(-1)^{k+1}}{k}\right), \quad \eta_n = \frac{E_q A\pi^2 n^2}{4L^2}$$

$$\zeta_n = \frac{2m}{n\pi}, \quad \alpha_n = \frac{2m\gamma L E_q}{n^3\pi^3\sigma_s^2}(1+(-1)^{n+1}), \quad k_n = \left(\frac{2\lambda^2}{\pi^4 n^4}\right)(1+(-1)^{n+1})^2$$

$$F_{yn} = \int_0^L YA\phi_n \,\mathrm{d}x, \quad F_{zn} = \int_0^L ZA\psi_n \,\mathrm{d}x \tag{3}$$

where YA and ZA are the external loads per unit length and ϕ_n and ψ_n are the out-of-plane and in-plane mode shapes, which are taken to be sinusoidal. Finally, the out-of-plane and in-plane natural frequencies, ω_{yn} and ω_{zn}, respectively, are given by

$$\omega_{yn} = \frac{n\pi}{L}\sqrt{\frac{\sigma_s}{\rho}}, \quad \omega_{zn} = \frac{n\pi}{L}\sqrt{\frac{\sigma_s}{\rho}(1+k_n)} \tag{4}$$

See Warnitchai et al. [23] for details of the derivation. Note that (i) these equations assume that the sag and end displacements are small, (ii) it is assumed that damping can be modelled as viscous with modal damping ratios ξ_{zn} and ξ_{yn} and (iii) this derivation assumes sinusoidal linear mode shapes which are approximated to the actual modeshapes in the presence of sag, resulting in minor errors for the odd in-plane modes [1] (however these modes are not relevant to the study reported here).

2.2. Step 2—Scaling and averaging

The cable is excited vertically at the bottom anchorage (point b) with amplitude Δ and angular frequency Ω. In this case the end conditions are $u_a = v_a = w_a = 0$, $u_b = \delta\sin\theta$, $w_b = \delta\cos\theta$ and $v_b = 0$, where $\delta = \Delta\cos(\Omega t)$ is the vertical anchorage displacement. No external forces are applied along the length of the cable.

In the simulation and experimental study presented in the next section the sag was such that $\omega_{z1} = 1.08\omega_{y1}$. The first in-plane mode is therefore sufficiently separated in frequency from the first out-of-plane mode for 2:1 resonance between the in-plane mode and the excitation (which is close to twice the first out-of-plane natural frequency) not to occur. The remaining modal frequencies have the theoretical relationships $\omega_{z2} = \omega_{y2} = 2\omega_{y1}$; we denote $\omega_2 = \omega_{z2} = \omega_{y2}$ and $\omega_1 = \omega_{y1}$ (experimental values are given in Section 3). From Eqs. (1) and (2), we can rewrite the modal equations of motion for the three modes being considered (assuming negligible response in other modes in the frequency range considered) as

$$\begin{aligned}
&\ddot{y}_1 + 2\xi_{y1}\omega_1\dot{y}_1 + \omega_1^2 y_1 + W_{11}y_1^3 + W_{12}y_1(y_2^2+z_2^2) + N_1\delta y_1 = 0\\
&\ddot{y}_2 + 2\xi_{y2}\omega_2\dot{y}_2 + \omega_2^2 y_2 + W_{21}y_2y_1^2 + W_{22}y_2(y_2^2+z_2^2) + N_2\delta y_2 = 0\\
&\ddot{z}_2 + 2\xi_{z2}\omega_2\dot{z}_2 + \omega_2^2 z_2 + W_{21}z_2y_1^2 + W_{22}z_2(y_2^2+z_2^2) + N_2\delta z_2 = B\ddot{\delta}
\end{aligned} \tag{5}$$

where $W_{nk} = v_{nk}/m$, $N_n = 2\eta_n\sin\theta/m$ and $B = \zeta_2\cos\theta/m$. This is a set of nonlinear equations with parametric excitation terms which we can examine via scaling and averaging.

Introducing the small parameter ε, we scale the equations such that they are in the standard Lagrange form, see Refs. [24,25]:

$$\ddot{x} + \omega_n^2 x = \varepsilon f(\dot{x}, x, t) \tag{6}$$

to reflect the fact that the response is dominated by the linear undamped response (a discussion of scaling is given in Bakri et al. [26]). The following transforms are made $\xi_{y1} \to \varepsilon\xi_{y1}$, $\xi_{y2} \to \varepsilon\xi_{y2}$,$\xi_{z2} \to \varepsilon\xi_{z2}$,

$(y_i, z_i) \to \varepsilon^{1/2}(y_i, z_i)$, $B \to \varepsilon^{1/2}B$ and $\delta \to \varepsilon\delta$, giving

$$\begin{aligned}
&\ddot{y}_1 + \omega_1^2 y_1 + \varepsilon(2\xi_{y1}\omega_1\dot{y}_1 + N_1\delta y_1 + W_{11}y_1^3 + W_{12}y_1[y_2^2 + z_2^2]) = 0\\
&\ddot{y}_2 + \omega_2^2 y_2 + \varepsilon(2\xi_{y2}\omega_2\dot{y}_2 + N_2\delta y_2 + W_{21}y_2y_1^2 + W_{22}y_2[y_2^2 + z_2^2]) = 0\\
&\ddot{z}_2 + \omega_2^2 z_2 + \varepsilon(2\xi_{z2}\omega_2\dot{z}_2 + N_2\delta z_2 + W_{21}z_2y_1^2 + W_{22}z_2[y_2^2 + z_2^2]) = \varepsilon B\ddot{\delta}
\end{aligned} \tag{7}$$

The forcing frequency is close to twice the first out-of-plane natural frequency. Therefore we write $\Omega = 2\omega_1(1+\mu)$ and then scale $\mu \to \varepsilon\mu$ such that $\Omega = 2\omega_1(1+\varepsilon\mu)$ in the scaled domain. Using this, taking into account that $\omega_2 = 2\omega_1$ and applying the time transform $\tau = (1+\varepsilon\mu)t$, we can write

$$\begin{aligned}
&y_1'' + \omega_1^2 y_1 + \varepsilon(2\xi_{y1}\omega_1 y_1' + N_1\delta y_1 - 2\mu\omega_1^2 y_1 + W_{11}y_1^3 + W_{12}y_1[y_2^2 + z_2^2]) = \mathcal{O}(\varepsilon^2)\\
&y_2'' + \omega_2^2 y_2 + \varepsilon(2\xi_{y2}\omega_2 y_2' + N_2\delta y_2 - 2\mu\omega_2^2 y_2 + W_{21}y_2y_1^2 + W_{22}y_2[y_2^2 + z_2^2]) = \mathcal{O}(\varepsilon^2)\\
&z_2'' + \omega_2^2 z_2 + \varepsilon(2\xi_{z2}\omega_2 z_2' + N_2\delta z_2 - 2\mu\omega_2^2 z_2 + W_{21}z_2y_1^2 + W_{22}z_2[y_2^2 + z_2^2] - B\delta'') = \mathcal{O}(\varepsilon^2)
\end{aligned} \tag{8}$$

where $\{\}'$ represents the derivative with respect to τ and we assume the higher-order terms with respect to ε are negligible.

We introduce the notation $\{x_{11},\ x_{22},\ x_{32}\} = \{y_1,\ y_2,\ z_2\}$ where the second subscript in x_{ij} represents whether the variable relates to a first or second mode. We also introduce the shorthand version for the equations in Eq. (8)

$$x_{ij}'' + \omega_j^2 x_{ij} = \varepsilon X_i \quad \text{for} \quad \{i,j\} = \{1,1\},\{2,2\},\{3,2\} \tag{9}$$

where the terms X_i may be derived by comparing Eqs. (8) and (9).

The equations are now in a form which can be averaged (see for example Refs. [24–26]). We apply transformations to x_{ij} in the form

$$x_{ij} = x_{ijc}\cos(\omega_j\tau) + x_{ijs}\sin(\omega_j\tau) \tag{10}$$

$$x_{ij}' = -\omega_j x_{ijc}\sin(\omega_j\tau) + \omega_j x_{ijs}\cos(\omega_j\tau) \tag{11}$$

Applying these transforms to Eq. (9) and applying the condition that the derivative of the right-hand side of Eq. (10) must equal the right-hand side of Eq. (11) for all three modes gives

$$x_{ijc}' = -\frac{\varepsilon}{\omega_j}\sin(\omega_j\tau)X_i, \quad x_{ijs}' = \frac{\varepsilon}{\omega_j}\cos(\omega_j\tau)X_i \tag{12}$$

From inspection of the equations in Eq. (12), it can be seen that the derivative terms of x_{ijc} and x_{ijs} are small and so over a short timespan x_{ijc} and x_{ijs} may be treated as constant [25]. We can therefore average equations (12) over an oscillation at frequency ω_1, treating the x_{ijc} and x_{ijs} terms within X_i as constant over the oscillation (taking the values x_{ijca} and x_{ijsa}, where subscript a indicates that they are approximate averaged values). Note that this averaging is applied to equations expressed in terms of scaled time τ, and is equivalent to averaging over two oscillation at excitation frequency Ω with respect to time t (since $\Omega t = 2\omega_1\tau$). During the averaging process many of the terms within X_i are averaged out indicating that although these terms cause oscillations in x_{ij} they do not affect the underlying amplitude trajectory of x_{ij}. Applying the averaging technique [24] gives the following equations for the averaged parameters:

$$\begin{aligned}
y_{1ca}' &= -\frac{\varepsilon}{\omega_1}\left(\xi_{y1}\omega_1^2 y_{1ca} + [\mu\omega_1^2 + \frac{N_1}{4}\Delta]y_{1sa} - \frac{3}{8}W_{11}y_{1sa}Y_{1a}^2 - \frac{1}{4}W_{12}y_{1sa}[Y_{2a}^2 + Z_{2a}^2]\right)\\
y_{1sa}' &= \frac{\varepsilon}{\omega_1}\left(\left[\mu\omega_1^2 - \frac{N_1}{4}\Delta\right]y_{1ca} - \xi_{y1}\omega_1^2 y_{1sa} - \frac{3}{8}W_{11}y_{1ca}Y_{1a}^2 - \frac{1}{4}W_{12}y_{1ca}[Y_{2a}^2 + Z_{2a}^2]\right)
\end{aligned}$$

$$
\begin{aligned}
y'_{2ca} &= -\frac{\varepsilon}{\omega_2}\left(\xi_{y2}\omega_2^2 y_{2ca} + \mu\omega_2^2 y_{2sa} - \frac{1}{4}W_{21}y_{2sa}Y_{1a}^2 - \frac{1}{8}W_{22}y_{2sa}[3Y_{2a}^2 + Z_{2a}^2] - \frac{1}{4}W_{22}z_{2sa}C_{2a}\right)\\
y'_{2sa} &= \frac{\varepsilon}{\omega_2}\left(\mu\omega_2^2 y_{2ca} - \xi_{y2}\omega_2^2 y_{2sa} - \frac{1}{4}W_{21}y_{2ca}Y_{1a}^2 - \frac{1}{8}W_{22}y_{2ca}[3Y_{2a}^2 + Z_{2a}^2] - \frac{1}{4}W_{22}z_{2ca}C_{2a}\right)\\
z'_{2ca} &= -\frac{\varepsilon}{\omega_2}\left(\xi_{z2}\omega_2^2 z_{2ca} + \mu\omega_2^2 z_{2sa} - \frac{1}{4}W_{21}z_{2sa}Y_{1a}^2 - \frac{1}{8}W_{22}z_{2sa}[3Z_{2a}^2 + Y_{2a}^2] - \frac{1}{4}W_{22}y_{2sa}C_{2a}\right)\\
z'_{2sa} &= \frac{\varepsilon}{\omega_2}\left(\mu\omega_2^2 z_{2ca} - \xi_{z2}\omega_2^2 z_{2sa} - \frac{1}{4}W_{21}z_{2ca}Y_{1a}^2 - \frac{1}{8}W_{22}z_{2ca}[3Z_{2a}^2 + Y_{2a}^2] - \frac{1}{4}W_{22}y_{2ca}C_{2a} - \frac{1}{2}B\Delta\omega_2^2\right)
\end{aligned}
\tag{13}
$$

where $Y_{1a}^2 = y_{1ca}^2 + y_{1sa}^2$, $Y_{2a}^2 = y_{2ca}^2 + y_{2sa}^2$, $Z_{2a}^2 = z_{2ca}^2 + z_{2sa}^2$ are the modal amplitudes, $C_{2a} = y_{2ca}z_{2ca} + y_{2sa}z_{2sa}$ represents cross coupling terms and Δ is the amplitude of vertical anchorage displacement, $\delta = \Delta\cos(\Omega t)$.

2.3. Step 3—Localised stability

Now we examine the first-order differential equations (13) to assess the stability boundary of the semi-trivial solution. The external excitation will lead directly to in-plane motion. With increasing excitation amplitude either of the out-of-plane modes can be excited, marking the boundary of the semi-trivial solution parameter space. To find the boundary of the semi-trivial solution in parameter space we examine the localised stability of each out-of-plane mode about zero response assuming that the other out-of-plane mode has zero amplitude.

For the first out-of-plane mode we can write

$$
\begin{Bmatrix} y'_{1ca} \\ y'_{1sa} \end{Bmatrix} = \varepsilon \begin{bmatrix} -\xi_{y1}\omega_1 & -\dfrac{N_1\Delta}{4\omega_1} - \mu\omega_1 + \dfrac{W_{12}Z_{2a}^2}{4\omega_1} \\ -\dfrac{N_1\Delta}{4\omega_1} + \mu\omega_1 - \dfrac{W_{12}Z_{2a}^2}{4\omega_1} & -\xi_{y1}\omega_1 \end{bmatrix} \begin{Bmatrix} y_{1ca} \\ y_{1sa} \end{Bmatrix} \tag{14}
$$

where we have set the second out-of-plane mode amplitudes to zero and neglected the higher-order y_{1ca} and y_{1sa} terms as we are considering the stability about the $y_{1a} = 0$ point. We note that this partially linearises the equations. However, the nonlinear internally excited $W_{12}Z_{2a}^2$-based terms remain. The resulting eigenvalues, χ (where we apply the scaling $\chi \to \varepsilon\chi$), are given by

$$
16\omega_1^2\chi^2 + 32\xi_{y1}\omega_1^3\chi + W_{12}^2Z_{2a}^4 - 8W_{12}\mu\omega_1^2Z_{2a}^2 + 16\omega_1^4(\mu^2 + \xi_{y1}^2) - N_1^2\Delta^2 = 0 \tag{15}
$$

Initially when the excitation amplitude is small (such that Δ and Z_{2a}^2 are small) the eigenvalues have negative real parts and hence the stable solution set is from zero excitation up to the boundary at which the real part of one of the eigenvalues is zero. This stability boundary is given by

$$
W_{12}^2Z_{2a}^4 - 8W_{12}\mu\omega_1^2Z_{2a}^2 + 16\omega_1^4(\mu^2 + \xi_{y1}^2) - N_1^2\Delta^2 = 0 \tag{16}
$$

Using the same technique for the second out-of-plane mode and noting that $\omega_2 = 2\omega_1$ and $W_{22} = 4W_{12}$, the local eigenvalue equation is given by

$$
16\omega_1^2\chi^2 + 64\xi_{y2}\omega_1^3\chi + 3W_{12}^2Z_{2a}^4 - 32W_{12}\mu\omega_1^2Z_{2a}^2 + 64\omega_1^4(\mu^2 + \xi_{y2}^2) = 0 \tag{17}
$$

As before, when the excitation amplitude is small the eigenvalues have negative real parts and hence the stable solution set is from zero excitation up to the boundary at which the real part of one of the eigenvalues is zero. When μ is negative (i.e. when the excitation frequency is below $2\omega_1$) the eigenvalues are stable for all Z. For positive μ the stability boundary is defined by

$$
3W_{12}^2Z_{2a}^4 - 32W_{12}\mu\omega_1^2Z_{2a}^2 + 64\omega_1^4(\mu^2 + \xi_{y2}^2) = 0 \tag{18}
$$

For this equation real positive solutions for Z_{2a}^2 only exist if $\mu \geqslant \sqrt{3}\xi_{y2}$, and if this condition is satisfied there are two real positive solutions for Z_{2a}^2 and hence two stability boundaries. For $\mu < \sqrt{3}\xi_{y2}$ the second out-of-plane mode is stable about the zero amplitude position for all Z_{2a} and hence for all excitation amplitudes Δ.

Finally to allow the calculation of the semi-trivial solution boundary we must derive an equation for Z_{2a} in terms of the excitation amplitude noting that just below a point on the solution boundary the out-of-plane modes have zero amplitude. We can therefore reduce the equations for the second in-plane mode in Eq. (13) to

$$\begin{aligned} z'_{2ca} &= -\frac{\varepsilon}{\omega_2}\left(\xi_{z2}\omega_2^2 z_{2ca} + \left[\mu\omega_2^2 - \frac{3}{8}W_{22}Z_{2a}^2\right]z_{2sa}\right) \\ z'_{2sa} &= \frac{\varepsilon}{\omega_2}\left(\left[\mu\omega_2^2 - \frac{3}{8}W_{22}Z_{2a}^2\right]z_{2ca} - \xi_{z2}\omega_2^2 z_{2sa} - \frac{1}{2}B\Delta\omega_2^2\right) \end{aligned} \tag{19}$$

Setting these equations to zero, the steady-state amplitude of oscillation of the second in-plane mode may we written as

$$16\omega_1^4 B^2\Delta^2 = 64\omega_1^4(\mu^2 + \xi_{z2}^2)Z_{2a}^2 - 48\omega_1^2\mu W_{12}Z_{2a}^4 + 9W_{12}^2Z_{2a}^6 \tag{20}$$

Solving Eq. (20) with Eqs. (16) and (18) allows the amplitude of excitation at which the boundary of stability occurs for the first (second out-of-plane) mode, to be found as a function of the support motion frequency. We first express the semi-trivial solution boundary equations, Eqs. (16) and (18), and the amplitude equation (20) in nondimensional form using the parameters:

$$\begin{aligned} \varepsilon_s &= \frac{\sigma_s}{E} \quad \gamma_\theta = \frac{\rho g L\cos(\theta)}{A\sigma_s} \\ \hat{Z}_{2a} &= \frac{Z_{2a}}{L} \quad \hat{\Delta} = \frac{\Delta}{L} \end{aligned} \tag{21}$$

Using these expressions and the equations in Eq. (3), the first out-of-plane boundary equation (16) may be written as

$$\pi^4\hat{Z}_{2a}^4 - 8\varepsilon_s\mu\pi^2\hat{Z}_{2a}^2 + 16\varepsilon_s^2(\mu^2 + \xi_{y1}^2) - \frac{144}{(12+\lambda^2)^2}\sin^2(\theta)\hat{\Delta}^2 = 0 \tag{22}$$

and the second out-of-plane boundary equation (18) as

$$3\pi^4\hat{Z}_{2a}^4 - 32\varepsilon_s\mu\pi^2\hat{Z}_{2a}^2 + 64\varepsilon_s^2(\mu^2 + \xi_{y2}^2) = 0 \tag{23}$$

where Irvine's parameter may be written as $\lambda^2 = \gamma_\theta^2/\varepsilon_s$. Finally the steady-state amplitude of oscillation of the second in-plane mode equation (20) may we written as

$$16\varepsilon_s^2\cos^2(\theta)\hat{\Delta}^2 = 64\pi^2\varepsilon_s^2(\mu^2 + \xi_{2z}^2)\hat{Z}_{2a}^2 - 48\pi^4\varepsilon_s\mu\hat{Z}_{2a}^4 + 9\pi^6\hat{Z}_{2a}^6 \tag{24}$$

(Note that when reversing the transforms $\xi_{y1} \to \varepsilon\xi_{y1}$, etc. the scaling factor ε cancels out.)

3. Stability boundaries: theory, simulation and experiment

The experiment consists of a 1.98 m long, steel cable which is inclined at 20° to the horizontal. The cable has a diameter of 0.8 mm and has a mass of 0.67 kg/m (in the experiments this is achieved by attaching lead weights at 60 mm interval). The static tension of the cable is 205 N. The experimental set-up is shown in Fig. 2. This gives nondimensional parameter values: $\varepsilon_s = 2.04 \times 10^{-3}$ and $\gamma_\theta = 59.7 \times 10^{-3}$ (giving $\lambda^2 = 1.74$). These were chosen to approximately match a typical full-scale bridge cable of length 400 m, mass per unit length 130 kg/m and tension 8000 kN [12].

MATLAB/Simulink was used in conjunction with a dSpace DS1104 RD controller board to implement an actuator controller and data acquisition system. The cable was dynamically excited using a electrically driven ball-screw actuator which applies a displacement to the cable anchorage point in the vertical direction. The instrumentation consisted of two load cells (aligned with the cable) to measure the static tension and the dynamic force acting at the top and bottom cable anchorages, one LVDT displacement transducer to be able to track and control the actuator movement and a digital incremental encoder used to control the initial

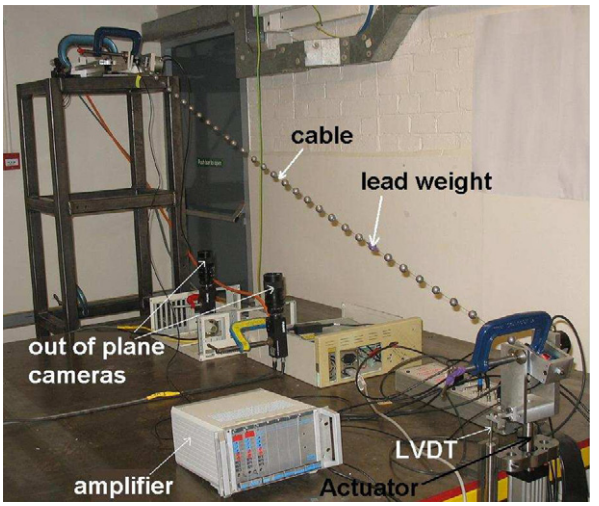

Fig. 2. Experimental set-up.

Table 1
Cable natural frequencies

	ω_{y1} (Hz)	ω_{y2} (Hz)	ω_{z1} (Hz)	ω_{z2} (Hz)
Experimental	4.40	8.76	4.72	8.77
Theoretical	4.41	8.81	4.71	8.81

inclination of the cable. A high-speed vision system [22] was used to measure the cable motion at nine different points both in-plane and out-of-plane.

Natural frequencies and damping ratios were identified experimentally using free vibration tests. The natural frequencies agreed well with the theoretical values (Eq. (4)) and are summarised in Table 1. The modal damping ratios over the range of oscillation amplitudes of interest were estimated to be approximately $\xi = 0.2\%$ for all three modes.

3.1. Theoretical stability boundaries

The theoretical stability boundaries in terms of the normalised excitation amplitude Δ/L and the corresponding normalised amplitude of the second in-plane mode at the out-of-plane Z_{2a}/L for a normalised excitation frequency Ω/ω_2 are found by numerically solving Eqs. (20) and (16) (or the nondimensional Eqs. (22) and (24)) via iteration for the first out-of-plane mode and Eqs. (20) and (18) (or Eqs. (23) and (24)) for the second out-of-plane mode.

The boundaries, in terms of the normalised excitation amplitude, are shown in Fig. 3. For the first out-of-plane mode there is a single boundary, for excitation levels below this boundary the zero response of the out-of-plane mode is stable and above it the zero response is unstable. For the second out-of-plane mode there are two stability boundaries for $\mu \geqslant \sqrt{3}\xi$ (corresponding to $\Omega/\omega_2 \geqslant 1 + \sqrt{3}\xi$). At low excitation levels, the mode is stable about zero amplitude response. Then with increasing Δ the lower boundary line is crossed and a response in the second out-of-plane mode is expected. If Δ is increased further, so that the second boundary level is crossed, the zero amplitude modal response becomes stable again.

3.2. Simulated stability boundaries

Simulation results were generated by using the Matlab ode45 timestepping routine applied to Eq. (5). By inspection of Eqs. (5), it can be seen that even when one of the out-of-plane modes is unstable about zero

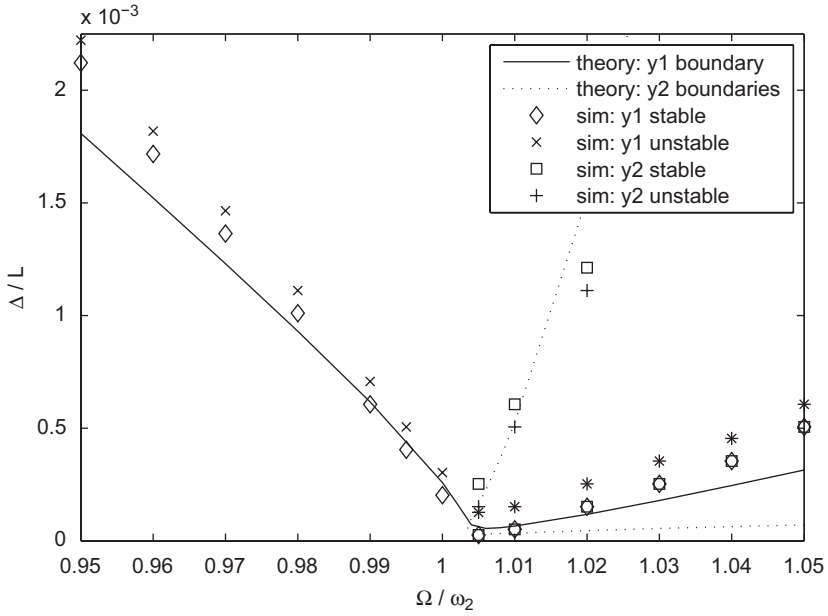

Fig. 3. Stability boundaries: theoretical and simulated (with zero initial conditions for the second in-plane mode). Note overlaid + and × symbols appear as ∗.

amplitude no modal responses occur unless there is an external disturbance. Therefore, in the simulations the excitation is run for 25 s, by which time the directly excited second in-plane mode response is approximately steady state. At 25 s a disturbance, in the form of a 0.02 s, 0.1 mm/s amplitude pulse, is applied to the velocity of both of the out-of-plane modes, and the stability of the modes is assessed. This is done for a range of excitation amplitudes with increments of 0.2 mm (or $\Delta/L = 1.01 \times 10^{-4}$). As an example, Fig. 4 shows the modal responses when the system is excited at a frequency of $\Omega/\omega_2 = 0.97$ for two amplitudes, 2.7 and 2.9 mm, which correspond to stable and unstable y_1 mode responses, respectively (y_2 is stable for both cases).

Simulation of stability boundary results in which the initial conditions for the second in-plane mode are zero are shown in Fig. 3. For each value of Ω/ω_2 excitation amplitudes (with a resolution of 0.2 mm) either side of the observed modal stability boundaries are marked, for example for $\Omega/\omega_2 = 0.97$, considering the y_1 mode, 2.7 mm excitation is marked as stable and 2.9 mm as unstable. From this figure, for the first out-of-plane mode it can be seen that there is good agreement between the theory and the simulations in the region $0.98 \leqslant \Omega/\omega_2 \leqslant 1$. For $\Omega/\omega_2 \leqslant 0.98$ the agreement deteriorates. This is due to the scaling in which it was assumed that Δ and μ were small. There is no instability in the second out-of-plane mode for $\Omega/\omega_2 \leqslant 1$ as indicated by the theory. For $\Omega/\omega_2 > 1$ there is good agreement for the upper second mode stability boundary (with the same deterioration at larger values of Δ) even though there is significant response of the first out-of-plane mode at these excitation levels. However, the simulations do not agree well with the theory for the lower second mode and the first mode stability boundaries for $\Omega/\omega_2 \geqslant 1.01$. The reason for this disagreement is that the lower stability boundary does not correspond to the zero initial condition solution computed using the simulation. To see this, consider the equation for the amplitude of the second mode in-plane response (with zero response in the other modes), Eq. (20), from which

$$\frac{\mathrm{d}\Delta}{\mathrm{d}Z_{2a}} = \frac{Z_{2a}}{16\omega_1^4 B^2 \Delta}\left(64\omega_1^4(\mu^2 + \xi_{z2}^2) - 96\omega_1^2 \mu W_{12} Z_{2a}^2 + 27 W_{12}^2 Z_{2a}^4\right) \tag{25}$$

There are positive real values of Z_{2a} that satisfy $\mathrm{d}\Delta/\mathrm{d}Z_{2a} = 0$ if $\mu \geqslant \sqrt{3}\xi_{z2}$. This indicates that there are multiple solutions for Z_{2a} for a given Δ for $\mu \geqslant \sqrt{3}\xi_{z2}$, i.e. the curve has a fold. Using Eq. (20), an example relationship between Δ and Z_{2a} is shown in Fig. 5 for the case where $\Omega/\omega_2 = 1.03$. The points at which the

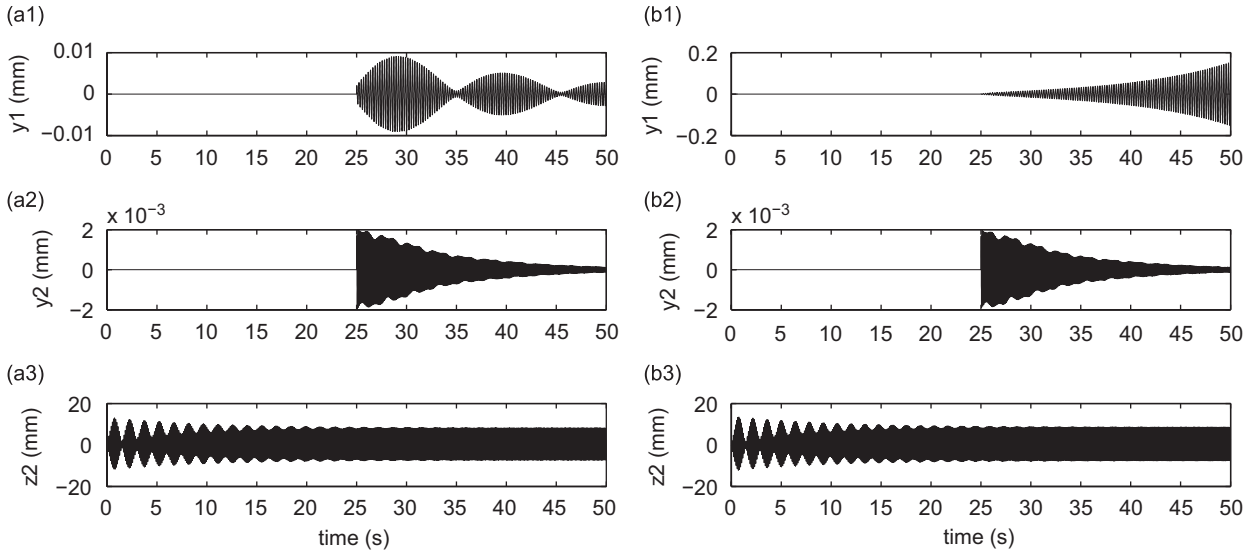

Fig. 4. Simulation time responses, $\Omega/\omega_2 = 0.97$, with excitation amplitudes of (a) 2.7 and (b) 2.9 mm.

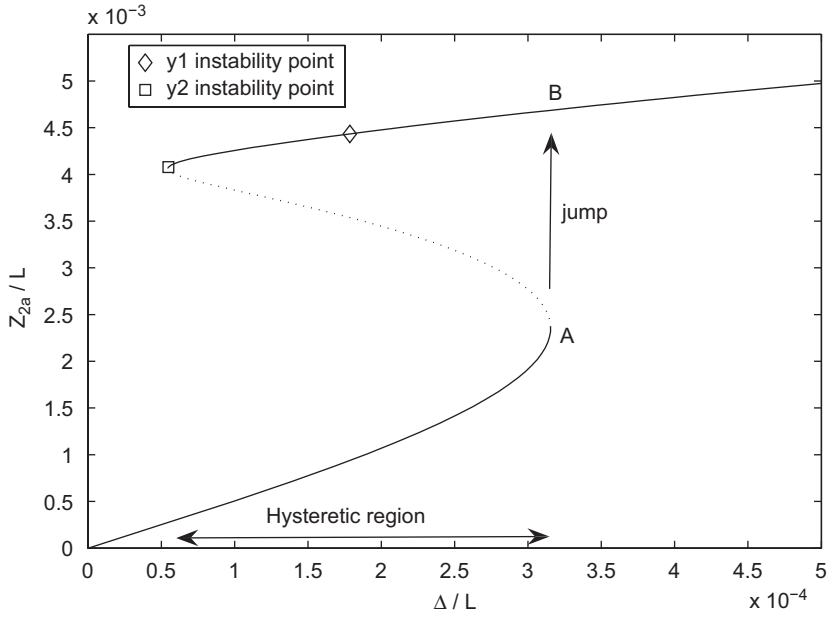

Fig. 5. Response of the second in-plane mode (assuming other modes remain stable) when excited at frequency $\Omega/\omega_2 = 1.03$ and amplitude Δ.

out-of-plane modes become unstable according to theory are indicated on the curve. The region of the curve represented by the dashed line is unstable. This may be shown by rewriting Eq. (19) in matrix form:

$$\mathbf{Z}'_{v2a} = f(\mathbf{Z}_{v2a}) \simeq f(\bar{\mathbf{Z}}_{v2a}) + (\mathbf{Z}_{v2a} - \bar{\mathbf{Z}}_{v2a}) Df(\hat{\mathbf{Z}}_{v2a}) \tag{26}$$

where $\mathbf{Z}_{v2a} = \{z_{2ca},\ z_{2sa}\}^{\mathrm{T}}$ and $Df(x)$ is the Jacobian of $f(x)$. The stability of the response is governed by the eigenvalues of the Jacobian evaluated at the possible equilibrium points, $\bar{\mathbf{Z}}_{v2a}$, such that $f(\bar{\mathbf{Z}}_{v2a}) = 0$, i.e. along the line governed by Eq. (20). (The instability point for the second out-of-plane mode occurs on a stable part of the Δ against Z_{2a} curve.) In the hysteretic region, where there are two stable solutions for the amplitude of the second in-plane response, simulations with zero initial conditions are attracted to the low-amplitude

solution. Therefore, instability in the out-of-plane modes only occurs when the excitation amplitude Δ exceeds the lower saddle-node bifurcation (point A in Fig. 5), at which point the amplitude of the second in-plane mode jumps to the larger solution curve, point B in Fig. 5. This higher solution is beyond the instability points of the two out-of-plane modes (i.e. point B is to the right of the instability points for both the out-of-plane modes in Fig. 5). So both modes go unstable at the jump from the lower bifurcation point (i.e. from A to B as indicated by the arrow in Fig. 5). From Eq. (25) the saddle-node bifurcation (point A) occurs when

$$Z_{2a}^2 = \frac{8\omega_1^2\mu}{9W_{12}}\left(2 - \sqrt{1 - 3\left(\frac{\xi_{z2}}{\mu}\right)^2}\right) \tag{27}$$

The turning point can be calculated in terms of Δ using Eqs. (20) and (27) and results in good agreement with the simulation data. To simulate the theoretical instability boundary which exists at point B in Fig. 5, the system must oscillate at the larger Z_{2a} amplitude solution before the out-of-plane disturbance is applied. This was achieved in the numerical simulation by initially setting an excitation amplitude higher than the turning point value and reducing it to the desired level after 15 s. After 25 s a pulse disturbance was applied to the out-of-plane modes to test for modal instability about the zero response position. The simulation results are shown in Fig. 6. It can be seen that there is excellent agreement with the theoretical predictions.

3.3. Experimental stability boundaries

In the experimental tests it was found that a small amount of oscillation (around 1 mm amplitude) of the second out-of-plane mode was present throughout all tests. It is thought that this was due to asymmetry in the set-up. Growth in amplitude of this mode was not observed to take place before instability of the first out-of-plane mode. The system was allowed 400 periods of external excitation for the transient response to decay. After the 400 periods a disturbance was introduced, in the form of a slight impulse applied horizontally to the mid-span lead weight. The out-of-plane amplitude of oscillation was then monitored for a further 400 periods to ascertain the stability of the mode. This procedure was repeated for increasing amplitudes of excitation to

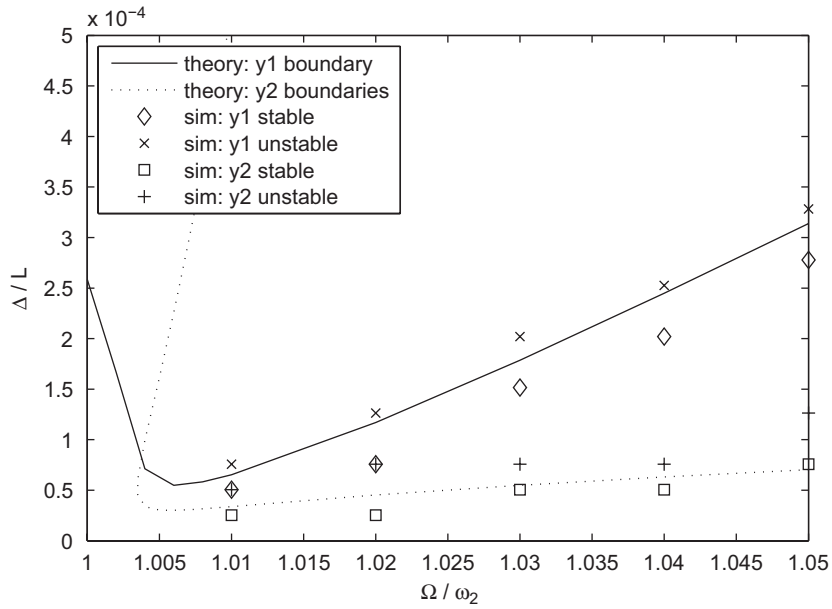

Fig. 6. Simulation stability points for $\Omega/\omega_2 \geqslant 1$ when the second in-plane response is at the higher amplitude solution.

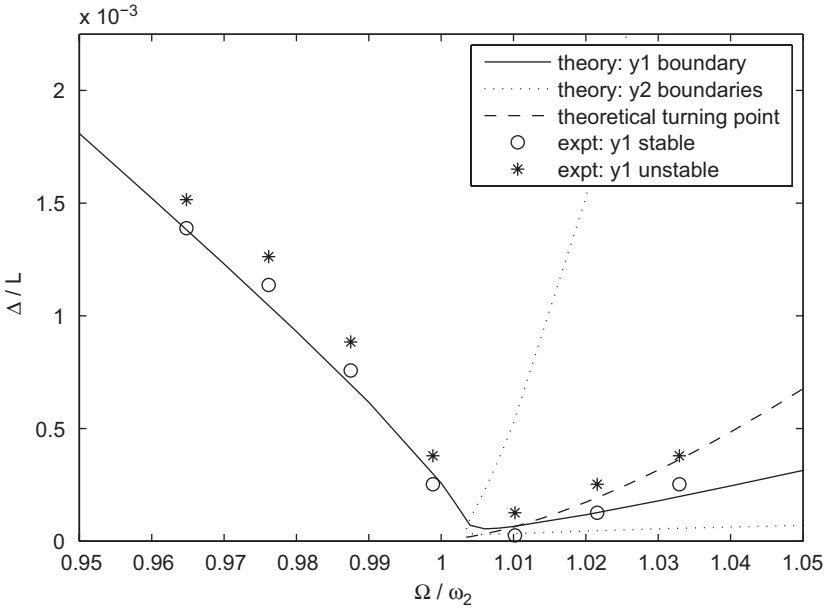

Fig. 7. Theoretical and experimental stability boundaries.

just beyond the instability point for a range of forcing frequencies up to $\Omega/\omega_2 = 1.04$. For $\Omega/\omega_2 > 1.04$ the first in-plane mode was excited, the stability of which is beyond the scope of our study.

Fig. 7 shows the experimental stability points, which also show very good agreement with the theoretical boundary for $\Omega/\omega_2 \leqslant 1.02$. For $\Omega/\omega_2 > 1.02$ the results diverge from the theoretical stability values; as with the simulations this is because the initial conditions of the second in-plane mode are zero and so the modal instability only occurs after the excitation amplitude exceeds the turning point defined by Eq. (27). It can be seen that this relationship agrees well with the experimental results for $\Omega/\omega_2 > 1.02$.

4. Discussion

There is very good agreement between the simulation and experimental observations presented in the previous section and the new theoretical model. We have demonstrated how the out-of-plane modes can go unstable at the theoretical stability boundaries defined by Eqs. (16) and (19) for the first out-of-plane mode and by Eqs. (18) and (19) for the second out-of-plane mode. When $\Omega/\omega_2 \geqslant 1 + \sqrt{3}\xi_{z2}$ a hysteretic region exists and there are two stable solutions for Z_{2a}. This fold in the relationship between Z_{2a} and Δ can have the effect of raising the excitation level required for the onset of vibrations in the out-of-plane modes as the instability can occur on the upper Z_{2a} branch. This raised excitation level can be calculated by considering the turning point in the relationship between Z_{2a} and Δ by solving Eqs. (20) and (27). We note that in the region where the turning point is below the theoretical stability boundaries, see Fig. 7, the Δ required for instability of the semi-trivial solution is governed by the theoretical stability boundary rather than the turning point relationship and hence the theoretical stability boundaries are conservative.

Currently the most widely used stability curve when studying 2:1 resonance is the one presented by Lilian and Pinto da Costa [2], which is used in practical bridge design recommendations, such as those produced by Setra [27], to provide guidance as to whether the expected cable anchorage motions would be large enough to initiate parametrically excited vibrations. The equations of the stability boundary in both works are found from a linear one-degree-of-freedom Mathieu-Hill-type equation. Since they reduce the study to a single degree of freedom they calculate y_1 and y_2 boundaries separately, the first excited in 2:1 resonance, the second in 1:1 resonance (due to external support excitation rather than internal resonance with the second in-plane mode). For the y_1 mode excited close to 2:1 resonance, Lilien and Pinto da Costa [2] states that the stability

boundary is given by

$$\hat{\Delta} = 2\frac{\varepsilon_s}{\sin(\theta)}\sqrt{\left[\left(\frac{\Omega}{2\omega_1}\right)^2 - 1\right]^2 + 4\xi^2\left[\frac{\Omega}{2\omega_1}\right]^2}. \tag{28}$$

An equivalent expression is given by Setra [27] which is virtually the same for $\Omega/(2\omega_1) \approx 1$. The minimum excitation amplitude at which parametric resonance occurs is hence $\hat{\Delta} = 4\xi\varepsilon_s/\sin(\theta)$ when $\Omega/(2\omega_1) = 1$, i.e. $\mu = 0$.

Fig. 8 shows a comparison of the y_1 mode instability boundary using the analytical model presented in this paper and the relationship proposed by Lilien and Pinto da Costa [2]. It can be seen that the minimum excitation to cause instability of the zero-amplitude response solution in the first out-of-plane mode occurs at $\Omega/\omega_2 = 1$ from the equations proposed by Lilien and Pinto [2] and Setra [27]. In contrast, the equations derived in this paper, Eqs. (16) and (19), which have been verified experimentally in Section 3, predict that the minimum excitation amplitude occurs away from resonance although the minimum amplitude remains approximately the same. In addition, the excitation amplitude to induce a response in the y_1 mode is significantly less than that predicted by Lilien and Pinto [2] and Setra [27] for frequencies above resonance. This shifting of the minimum and the reduction in amplitude of the higher frequency sides of the stability boundary are a direct consequence of the hardening that cables experience due to the geometric cubic nonlinearity from concurrent vibrations in the second in-plane mode. This nonlinearity is not taken into account in previous stability models, such as Refs. [2,27], and as a result the match with experimental data (as shown in the previous section) will be reduced. The reduction in amplitude of the curve shows clearly that parametric resonance can occur for much smaller anchorage motions that previously predicted [2,27] when $\Omega/\omega_2 > 1$.

Neither Ref. [2] nor Ref. [27] give a explicit equation to calculate the y_2 stability region considering the excitation via nonlinear coupling with the second in-plane mode. However the averaging technique used here has resulted in Eqs. (18) and (19), which match the experimental and simulation data well.

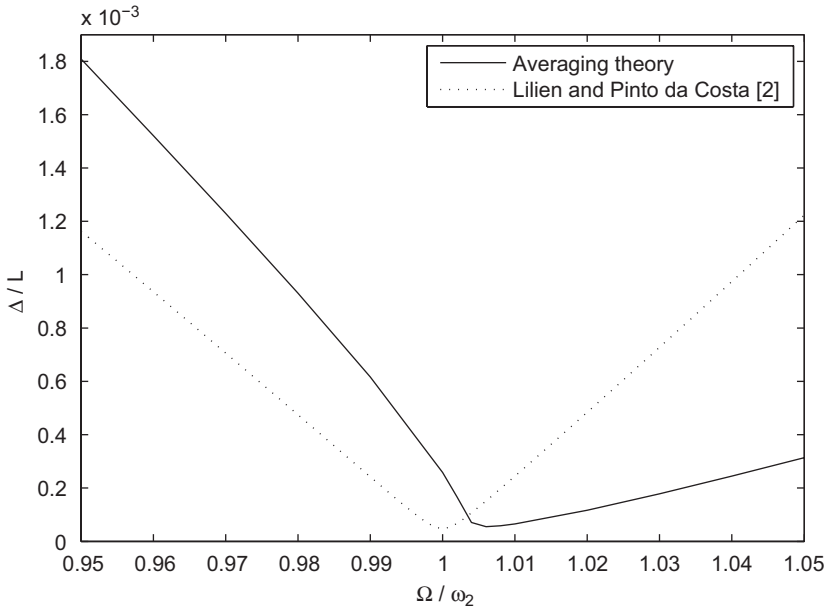

Fig. 8. First out-of-plane mode stability boundary proposed here (using averaging theory) compared to the boundary proposed by Lilien and Pinto da Costa [2].

5. Conclusions

In this paper we have presented an extended three-mode modal for the vibration of an inclined cable with vertical harmonic support excitation at the lower end of the cable. By including the model coupling terms, and using averaging, the three mode model has been used to explain some subtle dynamic behaviour which occurs around the 2:1 internal resonance of the in and out-of-plane modes. In particular the effect of the hysteretic jump on the numerical and experimental tracking of the lower stability branch for y_2 solutions has been explained in detail.

As part of this study a series of experimental tests were carried out using a scaled inclined cable with an actuator to give vertical excitation input at the lower support. Tests were carried out to observe the onset of oscillations in the out-of-plane modes, and these were compared with analysis and simulation from the three-mode model. Close agreement was found between the experimental and numerical results, giving a high degree of confidence in the extended three-mode model. This also demonstrates the importance of including the nonlinear coupling terms when studying the stability boundaries close to the 2:1 resonance region. Currently these coupling effects are not usually considered, but the results from this study show that the onset of oscillations in the out-of-plane modes can occur at lower amplitudes of excitation than predicted by previous models without coupling.

Acknowledgements

The authors would like to acknowledge the support of the EPSRC: Alicia Gonzalez-Buelga is supported by EPSRC Grant GR/S49780, David Wagg and John Macdonald via Advanced Research Fellowships and support was provided by EPSRC Grant GR/T28270/01.

References

[1] A.H. Nayfeh, P.F. Pai, *Linear and Nonlinear Structural Mechanics*, Wiley, New York, 2004.
[2] J.L. Lilien, A. Pinto da Costa, Vibration amplitudes caused by paramteric excitation of cable-stayed structures, *Journal of Sound and Vibration* 174 (1) (1994) 69–90.
[3] H.M. Irvine, *Cable Structures*, MIT Press, Cambridge, MA, 1981.
[4] W. Szemplinska-Stupnicka, The generalized harmonic balance method for determining the combinations resonance in the parametric dynamic systems, *Journal of Sound and Vibration* 58 (1978) 347–361.
[5] K. Takahashi, An approach to investigate the instability of the multiple-degree-of-freedom parametric dynamic systems, *Journal of Sound and Vibration* 78 (4) (1981) 519–529.
[6] R. Uhrig, On kinetic response of cables of cable-stayed bridges due to combined parametric and forced excitation, *Journal of Sound and Vibration* 165 (1) (1993) 185–192.
[7] E.S. Caetano, Indirect excitation of stays on cable-stayed bridges, Fourth International Symposium on Cable Dynamics, Montreal, Canada, 2001, pp. 129–136.
[8] K. Takahashi, Dynamic stability of cables subjected to an axial periodic load, *Journal of Sound and Vibration* 144 (2) (1991) 323–330.
[9] V. Gattulli, M. Lepidi, Nonlinear interactions in the planar dynamics of cable-stayed beam, *International Journal of Solids and Structures* 40 (2003) 4729–4748.
[10] Y. Fujino, P. Warnitchai, B.M. Pacheco, An experimental and analytical study of autoparametric resonance in a 3DOF model of a cable-stayed-beam, *Nonlinear Dynamics* 4 (1993) 111–138.
[11] C.T. Georgakis, J.H.G. Macdonald, C.A. Taylor, Non-linear analysis of wind-induced cable-deck interaction, *IABSE Conference Cable-supported Bridges*, Seoul, South Korea, IABSE Reports, 84, Paper 330, 2001.
[12] R. Lorenzo, Modelling of Cable–Structure Interaction in Cable-stayed Bridges and Examination of Their Parametric Response Under Stochastic Loading, PhD Thesis, University of Bristol, 2006.
[13] C.T. Georgakis, C.A. Taylor, Nonlinear dynamics of cable stays, part 1: sinusoidal cable support excitation, *Journal of Sound and Vibration* 281 (2005) 537–564.
[14] N.C. Perkins, Modal interactions in the non-linear response of elastic cables under parametric external excitation, *International Journal of Non-linear Mechanics* 27 (2) (1992) 233–250.
[15] F. Benedettini, G. Rega, R. Alaggio, Non-linear oscillations of a nonlinear model of a suspended cable, *Journal of Sound and Vibration* 182 (1995) 775–798.
[16] V.N. Pilipchuk, R.A. Ibrahim, Nonlinear modal interactions in shallow suspended cables, *Journal of Sound and Vibration* 227 (1) (1999) 1–28.

[17] H.N. Arafat, A.H. Nayfeh, Nonlinear responses of suspended cables to primary resonance excitations, *Journal of Sound and Vibrations* 266 (2003) 325–354.
[18] G. Rega, Nonlinear vibrations of suspended cables—part 1: modeling and analysis, *Applied Mechanics Review* 27 (6) (2004) 443–478.
[19] G. Rega, W. Lacarbonara, A.H. Nayfeh, C.M. Chin, Multiple resonances in suspended cables: direct versus reduced order models, *International Journal of Nonlinear Mechanics* 34 (1999) 901–924.
[20] R. Alaggio, G. Rega, Characterizing bifurcations and classes of motion in the transition to chaos trough 3D-tori of a continuous experimental system in solid mechanics, *Physica D* 137 (2000) 70–93.
[21] G. Rega, R. Alaggio, Spatio-temporal dimensionality in the overall complex dynamics of an experimental cable/mass system, *International Journal of Solids and Structures* 38 (2001) 2049–2068.
[22] J.H.G. Macdonald, C.A. Taylor, B.T. Thomas, E.L. Dagless, Real time remote monitoring of dynamic displacements by computer vision, *Sixth Society for Earthquake and Civil Engineering Dynamics Conference*, 1998, pp. 389–396.
[23] P. Warnitchai, Y. Fujino, T. Susumpow, A nonlinear dynamic model for cables and its application to a cable structure-system, *Journal of Sound and Vibration* 187 (4) (1995) 695–712.
[24] A. Tondl, T. Ruijgrok, F. Verhulst, R. Nabergoj, *Autoparametric Resonance in Mechanical Systems*, Cambridge University Press, Cambridge, 2000.
[25] F. Verhulst, *Nonlinear Differential Equations and Dynamical Systems*, Springer, Berlin, 1996.
[26] T. Bakri, R. Nabergoj, A. Tonel, F. Verhulst, Parametric excitation in non-linear dynamics, *International Journal of Non-Linear Mechanics* 39 (2004) 311–329.
[27] Setra, Cable Stays; Recommendations of French Interministerial Commission on Prestressing, Center des Techniques des Ouvraes d'Art, Bagneux Cedex, France, 2002, pp. 93–96.